Measurement Uncertainty, Channel Simulation, and Disturbance Characterization of an Over-the-Air Multi-Probe Setup for Cars at 5.9 GHz

Nilsson, Mikael; Hallbjörner, Paul; Arabäck, Niklas; Bergqvist, Björn; Abbas, Taimoor; Tufvesson, Fredrik

Published in:
IEEE Transactions on Industrial Electronics

DOI:
10.1109/TIE.2015.2475423

2015

Measurement Uncertainty, Channel Simulation, and Disturbance Characterization of an Over-the-Air Multi-Probe Setup for Cars at 5.9 GHz

Mikael G. Nilsson*‡, Paul Hallbjörner†, Niklas Arabäck†, Björn Bergqvist‡, Taimoor Abbas* and Fredrik Tufvesson*
*Lund University, Dept. of Electrical and Information Technology, Box 118, SE-221 00 Lund, Sweden
‡Volvo Car Corporation, SE-405 31 Göteborg, Sweden
†SP Technical Research Institute of Sweden, Box 857, SE-501 15 Borås, Sweden
email: mikael.nilsson@volvocars.com

***Abstract*—Over-the-air multi-probe setups provide an efficient way to characterize the performance of today's advanced wireless communication systems. In this paper the measurement uncertainty of such a setup using a car as a test object is characterized through three experiments: measurement system analysis, channel sounder measurements, and probe coupling measurements. Four issues were in focus for the analysis; precision, realization of the wireless communication channel, coupling between the probes, and the influence of the test object size. The analysis shows that a large test object such as a car in an over-the-air multi-probe ring will affect the measurement uncertainty, but only to a small degree. The measurement uncertainty expressed as expanded uncertainty was below +/-1dB, a level that would not violate best practice total uncertainty levels for comparable over-the-air methods.**

Keywords*—Over-the-Air, OTA, Multi-Probe, Multipath Propagation Simulator, MPS, Vehicle to Vehicle, V2V, Channel modelling, Measurement System Analysis, MSA, Expanded Uncertainty

I. Introduction

To increase road safety, vehicle manufacturers have until now used on-board sensors like radars, lasers and cameras to detect other vehicles or pedestrians. The next step would be to use the information from off-board sensors placed in surrounding vehicles. Data requiring low signal latency will be sent between the vehicles in the dedicated frequency band, 5.9 GHz, using the wireless communication standard IEEE 802.11p [1]. The wireless communication link will enable vehicles to communicate to each other and exchange information [2]. Wireless communications can make it possible to detect objects around the corners even if, e.g. the visual line-of-sight (LOS) is blocked, which is not possible for the sensors on the car today. Such information will allow the drivers to take actions even earlier than today to avoid collisions.

Research on vehicle-to-vehicle (V2V) and vehicle-to-infrastructure (V2I) communication started around a decade ago to support future intelligent transport systems (ITS). An important thing to investigate when using a new frequency band and communication protocol is the property of the wireless communication channel and how this will affect the system design and performance of the receivers. The access layer of 802.11p is based on 802.11a, which is designed primarily for indoor low mobility wireless local area networks. Therefore, new measurement campaigns are needed to analyze the influence of the outdoor wireless vehicular communication channel at high speeds. A number of measurement campaigns have been performed for this purpose, see e.g. [3] and the references therein. The channel characteristics derived from the measurements are used as design parameters when designing transceivers for the vehicles.

Measurement campaigns and drive tests are essential for channel characterization, but in the verification phase of an industrial project this kind of testing is expensive and time consuming. Therefore, to reduce the need of measurement campaigns when measuring the performance of cellular devices, the telecom industry has adopted Over-the-Air (OTA) testing [4] using reverberation chambers [5]–[7], OTA multi-probe testing [8]–[11], and verification by the two stage method [12]. The research area of OTA multi-probe testing for cellular devices is very active today. When the multiple-input multiple-output (MIMO) technology was introduced in the Evolved High-Speed Packet Access (HSPA+) OTA multi-probe testing showed big advantages. Costs were reduced, but also the complexity of the testing procedure.

The automotive industry can learn from the telecom industry by also applying OTA multi-probe testing on their products. A first step towards this, using a car with its antennas in an OTA multi-probe test system, is described in [13]. The current paper presents both experiments and characterization of the measurement uncertainty of an OTA multi-probe setup for cars at 5.9 GHz, in order to analyze if this kind of testing is also a way forward for the automotive industry.

II. Over-the-Air Multi-Probe Setups

A. State of the Art

Antenna measurements in anechoic chambers or at outdoor open area test sites are well established since the early days of wireless communication. Usually, there is only one probe to sample the field from the test object. Turntables then rotate the test object during test in order to cover several angles, but still only one direction at a time. An alternative, or complement to rotating the test object, is to have many probes, and switch between them [14]. Whether there are one or several probes in the setup, the need for an anechoic environment remains the same.

Active OTA signaling tests have much in common with antenna test measurements. A reason for using a multi-probe setup in signaling tests is to simulate the simultaneous propagation paths that exist in real life. The number of probes, their distances and angles relative to the test object, are parameters that need to be decided for optimal measurement accuracy and minimal cost [15], [16]. Most of the existing OTA multi-probe setups are using Plane Wave Synthesis (PWS) or Pre-Faded signals Synthesis (PFS) for creation of the propagation environment in the setup, [17]–[19]. With these synthesis methods the geometry based stochastic channel models can be simulated, which is important for testing mobile terminals.

The number of probes in a setup is typically 8 or 16, but up to 128 probes are also reported [14]. Taking into account the interference between the probes, the lower numbers are typically chosen. It has also been demonstrated that the electrical size of the test object is critical for the design of the probe array. Larger test objects necessitate a larger number of probes, if the goal is to achieve accurate PWS at the test zone [20]. However, if the goal is to simulate realistic wave propagation scenarios [21] and not aiming for either PWS or PFS, the number of probes should be chosen to match the actual multipath richness of the environment [22], [23]. Many signal environments are quite sparse, e.g. as few as four probes have been suggested for simulating an urban microcell in cellular networks [24] and typically a limited number of dominant multipath components have been observed in V2V/V2I communication channels, [25], [26].

The probes are typically placed in a circle around the test object, in the horizontal plane, and often with equal separation. Lately, so-called 3-D setups have been presented [27], [28], where the probes are placed at different elevation angles. The distance between test object and probes is usually limited by the size of the anechoic chamber. It is also limited upwards by the link budget of the setup. With a too small distance, on the other hand, the positioning of the test object can be critical, and unwanted coupling between the probes can be high. Setups for mobile handsets usually use a distance of 1-2 m. Setups for cars need of course a much larger distance but there are also other trade offs that need to be taken into account, this and other challenges are reported in [29], together with an overview of existing work ongoing in this area.

Cellular and vehicular communication systems use frequency bands over a wide range, so most presented setups use broadband antennas such as Vivaldi antennas or broadband dipoles to cover the desired frequencies. Dual polarized antennas, with orthogonal linear polarizations, are often used to be able to realize any average field polarization.

B. *Specific Issues*

As mentioned above, OTA testing has different prerequisites, e.g., depending on whether it is indoor or outdoor test facility, near field or far field test setup. The main contribution of this paper is to understand the uncertainty of OTA multi-probe tests for cars. Several experiments and analyzes were made to identify potential problems. It should be noted that there are many degrees of freedom in the setup, e.g., position of the car in the test zone, probe (transmit antenna) position and angle, see Fig. 1, which have to be considered in the analysis. Four issues were identified: 1) The precision; 2) The realization of the wireless communication channel; 3) The coupling between the transmit (TX) antennas; 4) The influence of the test object size. The latter issue could potentially be very critical since, to our best knowledge, there are no reports on OTA multi-probe testing on such a big test object as a car. In chapter III to V the issues are analyzed and discussed.

III. Measurement System Analysis

A. *Method*

The accuracy and the precision are important aspects of a measurement system. Accuracy is addressed by a good calibration process whereas precision is addressed by a good test procedure. The precision of the OTA multi-probe setup was characterized using a standard Gage R&R (Repeatability & Reproducibility) analysis [30]. Also the expanded uncertainty, u_e, [31] was calculated for the studied response metrics.

Gage R&R analysis is a standard technique to measure the precision of gages and other measurement systems. The analysis quantifies each component of variation:

- Repeatability: the variation in measurements taken by a single person or instrument on the same or replicate item and under the same conditions.
- Reproducibility: the variation induced when different operators, instruments, or laboratories measure the same part.
- Part-to-part variation.

Our Gage R&R (1) analysis is based on the analysis of variance (ANOVA) [30] which is a commonly used statistical model to analyze the difference between group means by comparing the variation 'Between Samples'to the variation 'Within Samples'. The Gage R&R is given by

$$G_{R\&R} = \frac{\sigma^2_{R\&R}}{\sigma^2_{Total}} \cdot 100, \tag{1}$$

where

$$\begin{aligned} \sigma^2_{Total} &= \sigma^2_{R\&R} + \sigma^2_{Part-to-part} \\ &= \sigma^2_{Repeatability} + \sigma^2_{Reproducibility} + \sigma^2_{Part-to-part} \end{aligned} \tag{2}$$

Gage R&R values less than 1 % is regarded as almost ideal, between 1-9 % it depends on the situation if the repeatability and reproducibility can be regarded as satisfactory, and above 9 % something needs to be done on the gages or measurement system to improve its precision [32].

The effects that give rise to uncertainty in measurements can be either random or systematic but instead of these terms the types of uncertainty contributions are grouped into two categories [33]:

- type A: those which are evaluated by statistical methods, repeated and reproduced measurements.
- type B: those which are evaluated by other means e.g., manufacturers' information/specification about instruments and components in the test set-up.
The classification into type A and type B is not meant to indicate that there is any difference in the nature of the components, it is simply a division based on their means of evaluation. In this paper the expanded uncertainty was evaluated according to type A. The expanded uncertainty value, u_e [31], is with 95% confidence given by

$$u_e = \pm k \frac{\sigma}{\sqrt{n}}, \tag{3}$$

where n is number of measurements performed on one part (the receive antenna) and k is the Students t-distribution coverage factor which is determined by n.

B. Test Setup and Object

For the OTA multi-probe setup for cars the Measurement System Analysis (MSA) process was using the test setup shown in Fig. 1. The test object was a Volvo S60 with four shark fin antennas (receive antennas) mounted on the roof, see Fig. 2. To get a high time resolution for the characterization of our test setup the S_{21} was measured using an Agilent 8753E Vector Network Analyzer (VNA) with a frequency sweep from 4.0 GHz to 6.0 GHz, IF bandwidth of 100 Hz, 1601 frequency points, and an output power of +10 dBm. The TX-antenna at position 1 (Fig.1) was used for the analysis and was directly connected to the VNA whereas four different receive (RX) antennas (Front, Left, Middle, Right) on the car were used throughout the measurements. The TX antennas were Vivaldi antennas [34] with a frequency span of 0.7-6.0 GHz. At 6.0 GHz the return loss is >12 dB, antenna gain is +3.8 dBi, and the beam width is 28° in the plane of the antenna (vertical polarization). The TX antenna height was 1.45 m for all antennas and the TX antennas were vertically polarized, placed pointing inwards along a circle with a radius of 5 m. The RX-antennas have a frequency span of 5850 MHz to 5925 MHz and return loss of 13 dB, the antenna gain patterns when the antennas are mounted on the roof are shown in Fig. 3. The used test sites were a tent at an open area, dimension = 20*12*6 m, with a turntable of 4 m in diameter and an anechoic chamber, dimension = 20.6*11.8*7.8 m, with a turntable of 9 m in diameter.

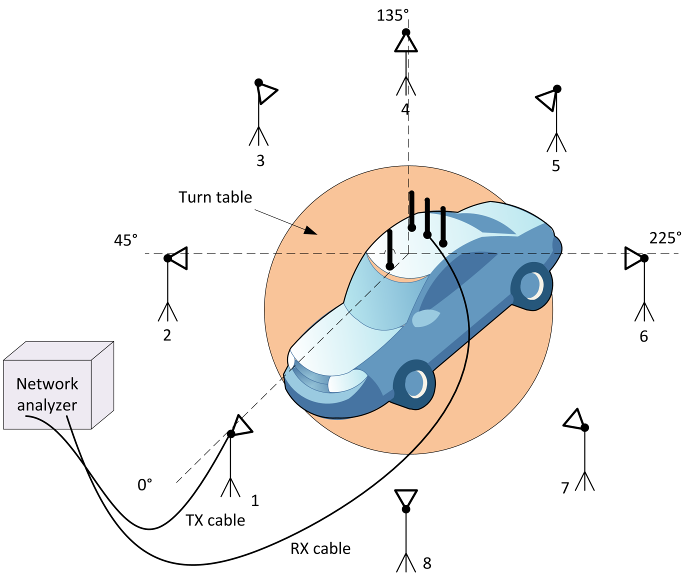

Fig. 1. Over-the-Air Multi-Probe Setup for the Measurement System Analysis (MSA).

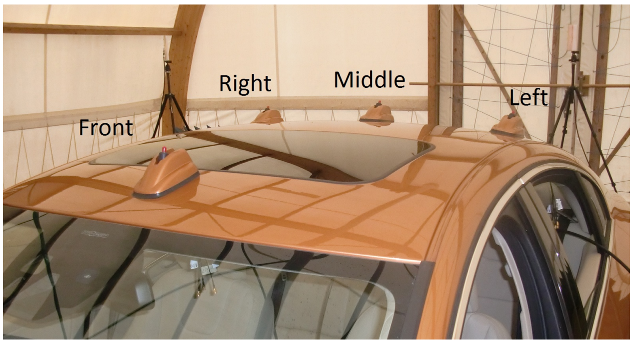

Fig. 2. The test object, a Volvo S60 with four shark fin antennas (RX antennas) mounted on the roof. Photo taken inside the tent at an open area.

C. Variability in test procedure

Four MSA's were performed to test different test sites and the sensitivity to variations of the measurement setup, see Table I. The measurements were performed a 0° of the RX antennas. Between each single measurement, as many factors

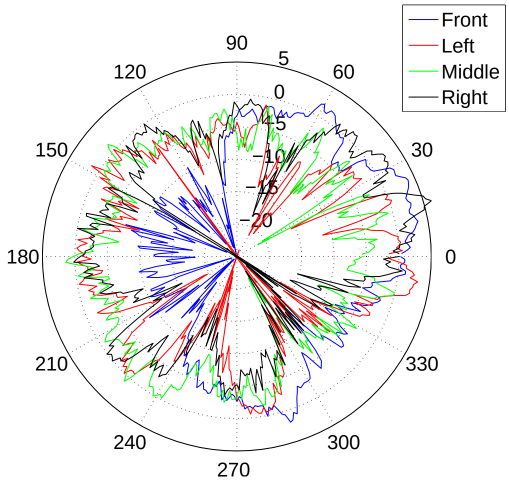

Fig. 3. Measured RX antenna pattern on vertical polarization, shark fins mounted on the Volvo S60. The front of the car is at 0° and antenna gain at this angle are for Front = 0.22 dBi, Left = -1.74 dBi, Middle = -5.91 dBi, and Right = -0.13 dBi.

TABLE I. MEASUREMENT SYSTEM ANALYSIS PROCESS

Name	RX antennas	Operators	Test site	No. of meas.
MSA 1	Front, Middle	2	Open area (tent)	20
MSA 2	Front, Middle	3	Anechoic chamber	30
MSA 3	Right, Middle, Left	2	Anechoic chamber	18
MSA 4	Right, Middle, Left	3	Open area (tent)	36

as practically possible should be changed and then set back to original settings before next measurement. Therefore the TX-antenna tripod was moved away from its position 1, the height was changed and the ball joint was loosened so the vertical alignment of the TX antenna towards the center of the car was changed. The cable between the VNA and the RX antenna was disconnected at the car side and the car was removed from its position and moved back to its position in the ring. The cable from the VNA to the TX antenna was, however, not disconnected. For MSA 2 and MSA 3 the position of the car was fixed since it was not practical to drive back and forth when performing the tests in an anechoic chamber. In this case the RX cable was only disconnected if the MSA procedure dictated changing RX antenna for that specific measurement.

D. Response Metrics

Before the analysis of the MSA can be performed the response metrics need to be defined. To identify the desired signal power vs. interference from the environment the impulse response was calculated using the inverse Fast Fourier transform (IFFT) of the measured transfer functions. From the impulse response, see Fig. 4, the power of the desired signal, here defined as the sum of powers from the first peak and the subsequent 0.1 μs, Signal, was calculated. This time duration is motivated by the inverse of the 10 MHz bandwidth used for IEEE 802.11p, as our goal is to evaluate the uncertainty of our test setup for such a system bandwidth. The metric Noise is determined by the average power level between

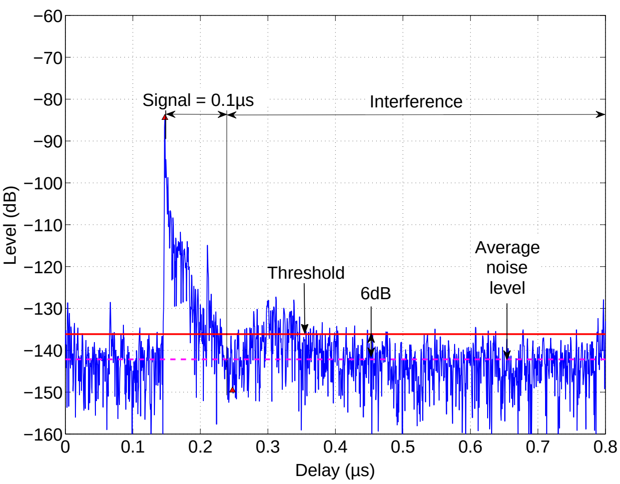

Fig. 4. Definition of response metrics based on measured impulse responses, here using the roof front antenna of a Volvo S60.

$0.5 - 0.7\,\mu s$ and the metric Interference, mainly reflections from the environment at the test site, is defined as the power of all the delay bins 6 dB above the average noise level having a delay 0.1 μs larger than the delay of the first peak. From these three response metrics also SNR, SIR and SINR were calculated and used as responses to be part of the analysis.

E. Result and Analysis

The statistics for the response Signal is shown in Table II. The results from an Anderson-Darling normality test on each RX antenna and for all MSAs show that the values on the response metric Signal has a Gaussian distribution with 95 % confidence, except for the Front antenna in MSA 2 due to that a cable was damaged and then replaced during this MSA. Therefore the mean and standard deviation values for Front antenna in MSA 2 are calculated without the measurements with the replaced cable.

TABLE II. MEAN AND STANDARD DEVIATION OF THE RESPONSE METRIC SIGNAL AT 0° FOR EACH RX ANTENNA.

RX ant.	MSA 1		MSA 2		MSA 3		MSA 4	
	μ $[dB]$	σ $[dB]$	μ $[dB]$	σ $[dB]$	μ $[dB]$	σ $[dB]$	μ $[dB]$	σ $[dB]$
Front	-77.93	0.84	-77.07	0.20	NA	NA	NA	NA
Left	NA	NA	NA	NA	-75.17	0.23	-86.44	0.36
Middle	-86.77	0.48	-86.13	0.41	-75.42	0.52	-86.08	1.01
Right	NA	NA	NA	NA	-72.99	0.30	-84.22	0.25

The three rear shark fin antennas have almost the same antenna gain in the front direction (position A = the front of the car pointing towards TX antenna 1) and the Front shark fin antenna has around 8 dB higher gain compared to the rear antennas, which is also seen in Fig. 5. The differences in the standard deviation between the different RX antennas is up to four times. For antenna Front it can be seen that there is an effect on the measured signal level by not moving the car between each measurement, since the standard deviation is less in MSA 2 compared with MSA 1. This effect is not seen between MSA 3 and MSA 4 since after having performed three MSAs we had in MSA 4 improved our skills to do the measurements and follow the test procedure. The reason why the standard deviation is that large in MSA 4 for antenna Middle compared to MSA 3 is that one of the operators did not follow the test procedure exactly during only one measurement on the RX antenna Middle, see Fig. 6, which directly had an effect on the standard deviation. The case was that this operator did not align the TX antenna towards the car as carefully as during the other measurements, the alignment error, we guess, could be in the order of 10°. The same statistical evaluations have been done for all responses but they are not presented in this paper due to space constraints, but next we discuss the results of the analysis.

For each of the four MSAs the Gage R&R per response metric has been calculated and the results are summarized in Table III. The u_e shown in the same table is the maximum value of the different RX antennas per response for each MSA.

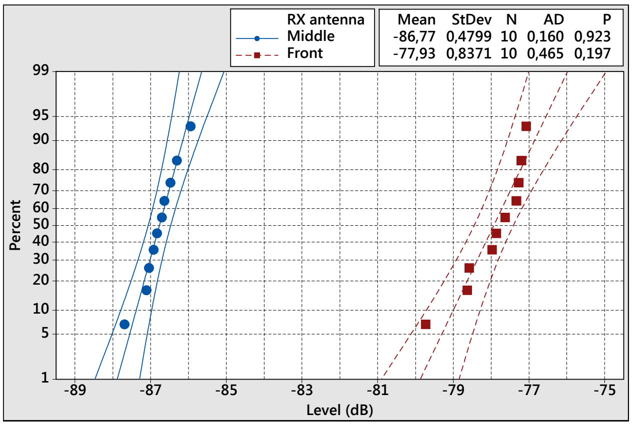

Fig. 5. MSA 1: Probability plot of the response metric Signal, fitted to normal distribution and with the 95 % confidence interval limits.

- Signal: Depending of the RX antenna gain at 0° the measurement system shows in general a low value on Gage R&R. In MSA 1 and 2 the Gage R&R values are really low since the difference of the RX antenna mean values are around 8 dB. In MSA 2 the last 7 measurements were re-measured due to the Front antenna cable was damaged during the measurement. If this would not have happened, the Gage R&R would have shown even better results since that could potentially introduce an offset of the output and that will affect the variance, as well as the Gage R&R.

In MSA 3 and 4 the difference between the RX antenna mean values are in the same range as the standard deviation. The measurement system can not resolve this small difference between the means and therefore the measurement system can not determine which RX antenna that is the best. The reason why MSA 3 shows much better result on Gage R&R compared to MSA 4 are two things. First, the variation in the results

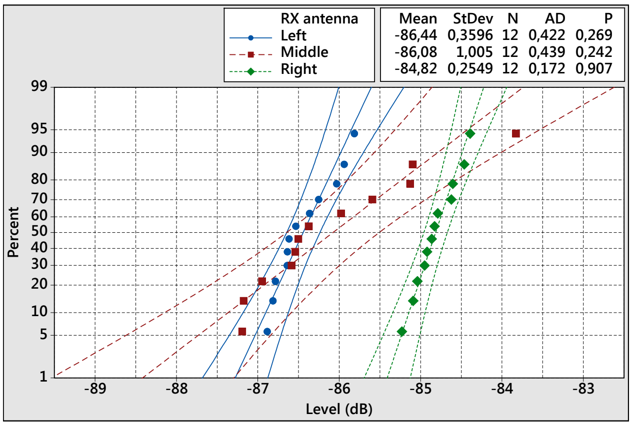

Fig. 6. MSA 4: Probability plot of the response metric Signal, fitted to normal distribution and with the 95 % confidence interval limits. The dot at around -83.8 dB for Middle antenna is the measurement were one operator did not align the TX antenna towards the car as careful as the other measurements.

TABLE III. GAGE R&R AND MAXIMUM EXPANDED UNCERTAINTY OF THE DIFFERENT RESPONSE METRICS.

Resp.	MSA 1		MSA 2		MSA 3		MSA 4	
	$G_{R\&R}$ [%]	u_e $[dB]$	$G_{R\&R}$ [%]	u_e $[dB]$	$G_{R\&R}$ [%]	u_e $[dB]$	$G_{R\&R}$ [%]	u_e $[dB]$
Signal	1.20	0.59	4.34	0.86	8.23	0.52	37.82	0.63
Noise	100	0.21	100	0.24	100	0.37	100	0.20
Interf.	42.06	0.55	7.48	0.88	100	0.65	23.26	0.26
SNR	1.09	0.57	3.40	0.73	9.07	0.58	41.81	0.69
SIR	4.51	0.79	14.67	0.20	31.46	0.92	19.22	0.65
SINR	1.99	0.65	2.16	0.36	9.27	0.60	24.31	0.64

is larger for all operators especially on the Middle antenna, see Fig. 6. Second, the earlier mentioned ‘mistake’ in MSA 4.

- Noise: The measurement system can not identify any difference in response metric Noise between the four RX antenna positions. The noise level is almost independent on the antenna in this frequency band, it is mostly dependent on the receiver noise figure. Therefore the noise level is always the same, resulting in a Gage R&R of 100. This response metric shall therefore not be used.

- Interference: Sometimes the power values of Interference are repeatable but sometimes not and this is shown by the fact that the Gage R&R is sometimes low and sometimes high for the response Interference. The measurement system can not resolve the response metric Interference, and this metric shall not be used.

- SNR: This response parameter has the same behavior as Signal since Noise is random, so SNR can be used as a response.

- SIR: Since Interference is not always repeatable, SIR shows the same behavior as Interference and shall not be used. At least this measurement system can not identify the small changes and it means that the Interference are not changing relative to the Signal during the measurements and therefore these are under control. SIR indicates also that all interference is received via the antenna. This response parameter could be valuable to analyze when the multi-probe setup is used at different locations to identify the interference environment, but these four MSAs does not show any trend between an open area (tent) and anechoic chamber.

- SINR: The power of Noise and Interference is around the same level. Signal is the dominating term in the response metric SINR and therefore SINR shows the same behavior as Signal. Hence SINR is a good response metric to use since both noise and interference are included SINR and both have an effect on the receiver.

The levels of expanded uncertainty, u_e, are between ± 0.36 dB and ± 0.86 dB for the three useful responses Signal, SNR and SINR. The MSAs show that the test procedure for the presented OTA multi-probe setup for cars regarding repeatability and reproducibility, $G_{R\&R}$, is under control when the difference of the performance of the different RX antennas are more than the expanded uncertainty. This is in-line with the ANOVA method, Analysis of Variance. As a comparison, the standard [35], setting requirements on open area test sites for radiated disturbance measurements, requires that the Normalized Site Attenuation (NSA) is deviating less than ± 4 dB from a theoretical value. With an u_e below ± 1 dB as reported in this paper the uncertainty contribution from the OTA multi-probe setup for cars at 5.9 GHz would not violate best practice total uncertainty levels for comparable methods.

IV. Channel Sounder Measurements

The main objective of the presented OTA multi-probe setup is to simulate a real radio environment for a car on the road. To show that this setup has these capabilities several measurements with the RUSK LUND channel sounder [36] were performed. In this paper we show that a uniform distribution of the TX antennas in azimuth with equal power can simulate an ideal Non-Line-of-Sight (NLOS) multipath environment with Rayleigh distributed amplitude. As an example a setup simulating a real life scenario, Highway convoy, was also measured with the channel sounder. The scattering function is then compared with one scattering function from a real highway measurement in Lund, Sweden.

A. Test Setup and Procedure

Switched-array MIMO measurements were performed by collecting the channel transfer function $H(f,t)$ from the TX antenna array to each RX antenna on the car using the channel sounder as seen in Fig. 7. The channel sounder had a center frequency of 5.75 GHz, a bandwidth of 240 MHz and measured at, N_f, 1537 frequency points within that bandwidth. The test signal length was 6.4 μs (one time sample), the gap between the time samples was also 6.4 μs and the total number of time samples, N_t, was 10,000. The same TX antennas and RX antennas were used as in the MSA, see chapter III-B. The delay and Doppler shifts for each TX antenna is generated by the Multipath Propagation Simulator (MPS) box and the

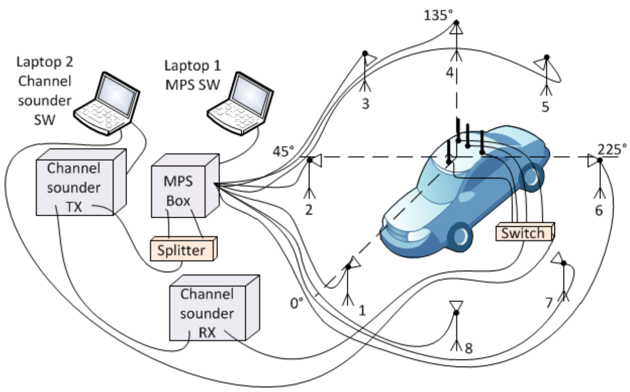

Fig. 7. Over-the-Air multi-probe setup for channel sounder measurements when having uniform distribution of the TX antennas.

TABLE IV. MPS parameters for the two test setups

TX ant.	Delay $[\mu s]$	Uniform Doppler $[Hz]$	Highway convoy Doppler $[Hz]$	Highway convoy Angle [deg]
1	0.12	398	10	180
2	0.20	353	745	5
3	2.31	254	-44	0
4	4.90	116	-756	185
5	0.28	-39	-770	170
6	0.57	-188	762	355
7	0.80	-309	98	180
8	1.16	-383	-257	250

settings for these two parameters are given in Table IV. The measurements were performed for two different setups: 1) uniform distribution of the eight TX antennas around the car with maximum 400 Hz U-shaped Jakes' Doppler spectrum represented with the discrete frequencies are more dense at the edges, and not symmetric to avoid periodic fading behavior [10]. This scenario is not so common in real life traffic situations. 2) a setup where the TX antennas are placed at specific angles to mimic a realistic highway convoy scenario with the corresponding delay and Doppler shifts. During measurement of one particular setup the parameters remained constant, neither the car nor the objects in the surrounding were moved, meaning that the large scale fading statistics remained constant and thus the considered measured response is assumed to be wide-sense stationary (WSS).

B. Result and Analysis

To analyze whether our OTA multi-probe setup with only eight uniformly distributed TX antennas has the capability to simulate an ideal NLOS multipath environment, we study the cumulative distribution function (CDF) and the autocorrelation function (ACF) of the received signal amplitudes for the Middle RX antenna.

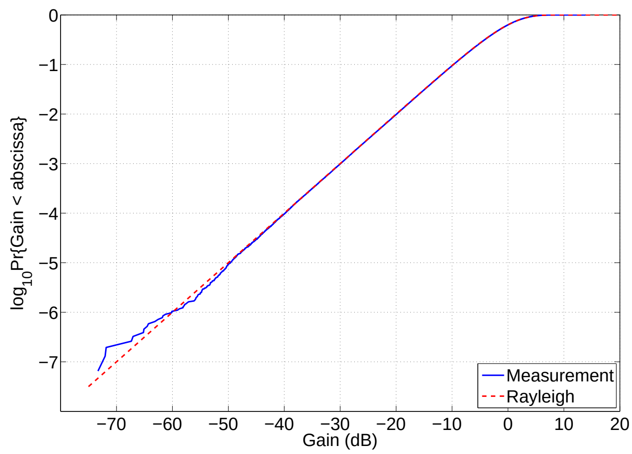

Fig. 8. Distribution of measured samples ($N_f \cdot N_t = 15,370,000$) compared with a theoretical Rayleigh distribution on a logarithmic scale. Used parameter for the theoretical Rayleigh, $\mu_1 = 0, \mu_2 = 0, \sigma_1 = 1$, and $\sigma_2 = 1$.

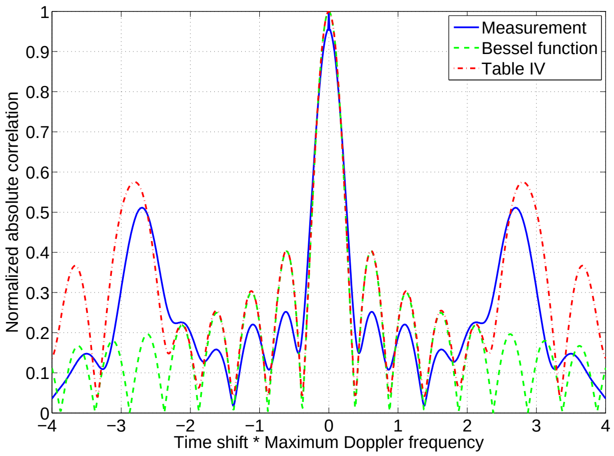

Fig. 9. Autocorrelation function in time domain normalized with the maximum Doppler frequency, 400 Hz. Three lines are shown: 1) the estimated measured autocorrelation function. 2) the zeroth order Bessel function of the first kind. 3) the inverse Fourier transform of eight discrete Doppler frequencies according to Table IV, all with equal amplitudes.

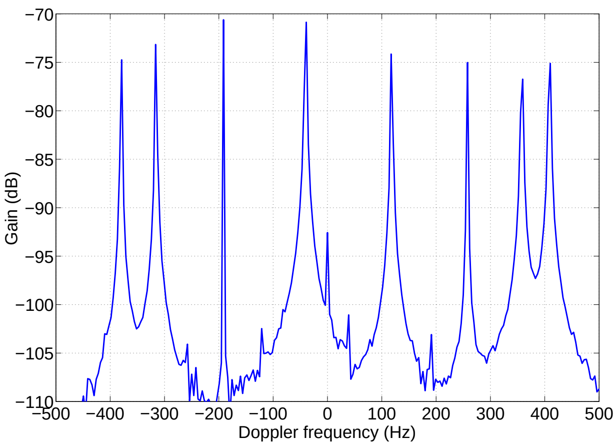

Fig. 10. Doppler spectrum from the measurement on the RX antenna, Middle, and according to Table IV with uniform setup.

The empirical CDF for the amplitude gain of the channel $|H(f,t)|$ is presented in Fig. 8 for a realization of $N_f \cdot N_t = 15,370,000$ samples. It can be seen in Fig. 8 that the measured data points have a good fit with the theoretical Rayleigh distribution down to probabilities around 10^{-5} and a reasonable fit down to 10^{-6}, which is within the expectation for such a sample size.

In a WSS random process with uniform 2D scattering and equally received power from all angles the ACF in time domain can be represented by a zeroth order Bessel function of first kind. With only eight discrete scatterers (TX antennas) and with Doppler shifts according to Table IV the correlation differs significantly from the Bessel function, see Fig. 9. There can be two reasons for this. First, only eight TX antennas with equal power cannot fully represent a U-shaped Jakes' Doppler spectrum. Second, in our case the received power from the

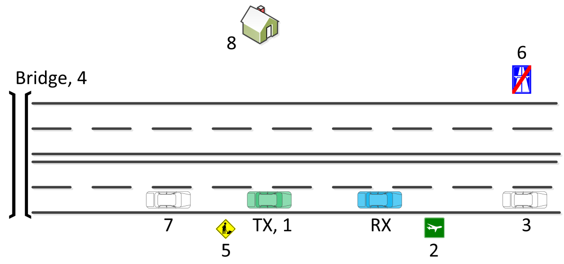

Fig. 11. Highway convoy scenario used in the OTA multi-probe setup according to Table IV. Where 1 represents the TX, 2, 5 and 6 represent the road signs, 3 and 7 represent the other vehicles, 4 represents the bridge and 8 represents a house at the roadside. The positions of the illustrated scattering objects are not scaled according to the distance.

eight paths are not equal, which is one of the prerequisites for the validity of the Bessel function.

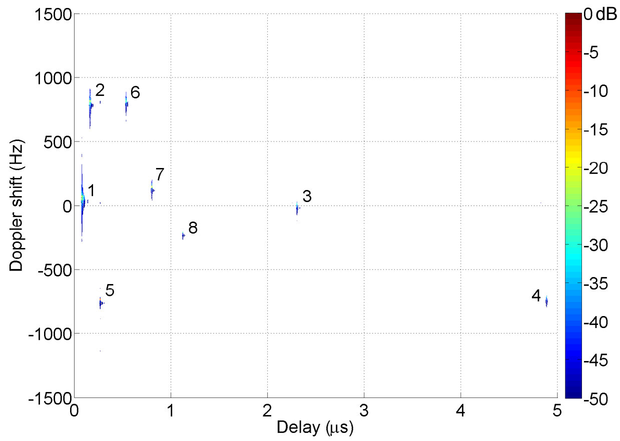

Fig. 12. Scattering function seen by the RX car of the highway convoy scenario presented in Table IV. The scatters are marked with the corresponding TX antenna numbers.

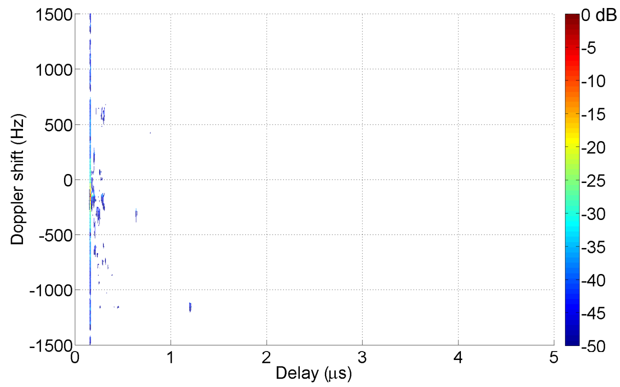

Fig. 13. Scattering function of one measurement made on a highway in Lund, Sweden [25].

The reason for the inequality is the RX antenna pattern variations, see Fig. 3, which effectively weights the powers of the different paths, resulting in a difference of up to 7 dB between the paths. Another theoretical comparison is also performed, the ACF estimated from the amplitude gain of the channel as $E[|H(f,t)||H(f,t+\tau)|]$ and the inverse Fourier transform of the discrete Doppler spectrum according to Table IV. In this case, the correspondence between the measured and theoretical ACF is reasonably good.

By this we are confident to say that a realization of an ideal NLOS multipath environment is possible to achieve with the presented OTA multi-probe setup. However, with typical variations in the test object radiation pattern, an ideal Jakes' Doppler spectrum environment for the entire channel cannot be realized with good accuracy. The ACF in the frequency domain is not meaningful to evaluate since the resolution in frequency domain is in the same range as the coherence bandwidth for the uniform setup.

For the second part we derived a theoretical highway convoy scenario with discrete scatterers, see Fig. 11, similar to the scenario from our measurement in Lund, Sweden [25]. The scattering function of the theoretical scenario implemented in the OTA multi-probe setup is shown in Fig. 12. An example from a corresponding scattering function measured in Lund is also presented in Fig. 13. Visual inspection of the two plots indicates that the presented OTA multi-probe setup can mimic a highway convoy scenario. The aim is however not to reproduce exactly the same multipath components, but rather the channel structure.

V. Probe Coupling Measurements

One source of disturbance in an OTA multi-probe setup is the TX antenna array reflecting signals from other TX antennas. Inevitably, each TX antenna will illuminate not only the test zone but also some of the other TX antennas, which will reflect the signal back into the test zone, and this can increase the uncertainty of the OTA multi-probe setup. The resulting disturbance level can be very high if there are many TX antennas and if they have a wide coverage. With only a few and more directive TX antennas the disturbance level can be negligible. One way to measure this disturbance level is to feed one TX antenna while measuring the power received by the other TX antennas and use the fact that a receiving antenna will re-radiate a power equal to the received power [37]. Our assumption is that the sum of the powers received by the other TX antennas therefore equals the disturbance level, D_r at the test zone (4), calculated as follows,

$$D_r = 10\log_{10}(2{\cdot}10^{S_{21}/10}+2{\cdot}10^{S_{31}/10}+2{\cdot}10^{S_{41}/10}+10^{S_{51}/10}). \quad (4)$$

These measurements should preferably be performed without any test object in the test zone.

Another source of disturbance in an OTA multi-probe setup is the test object itself. It will reflect and diffract the fields in the test zone. The same thing happens in real life, but in the OTA multi-probe setup, TX antennas are very close to the test object, so these disturbances might affect measurements in a way which has no relevance to the communication in real life. Large metal test objects such as cars are especially likely to cause disturbance of this kind. The magnitude of the reflections/diffractions from the car can be readily investigated by use of the different TX antennas in the setup. Measuring the transferred power between different pairs of the TX antennas, and comparing the results with and without the car present in the test zone, provides interesting information on the disturbance in question.

A. Test Setup and Procedure

Almost same setup as the MSA (see Fig. 1) was also used for these coupling measurements but the RX cable (see Fig. 1) was connected to the TX antenna 2 throughout 5. Five different test objects were used during this test, NO test object, Laptop (Dell Latitude E6420) standing on a wood and cardboard stand 1.05 m above ground, Volvo C30 (height 1.45 m), Volvo S60 (height 1.48 m) and a Volvo XC90 (height 1.78 m). For reasons of symmetry, only five transmission coefficients were measured, S_{21} to S_{51}. Measurements were performed with the same settings on the VNA as in the MSA except that the frequency span was 0.6 GHz to 6.0 GHz. Both vertical and horizontal polarization, respectively, on all TX antennas were measured with a height of 1.75 m and two positions of the car if this was the test object, position A the front of the car pointing towards TX antenna 1 and position B the front of the car pointing towards TX antenna 3. The measurements were performed inside the tent at the open area.

B. Result and Analysis

The measured average coupling levels with NO test object of the chosen frequency band 5.850 GHz to 5.925 GHz are shown in Table V, where "H-H" means that both transmitting and receiving TX antennas are horizontally polarized, and "V-V" means that both are vertically polarized. The reason to choose the frequency band 5.850 GHz to 5.925 GHz is that this is the frequency band that 802.11p modems normally operate at. As mentioned earlier, the disturbance level in the test zone is the sum of the received powers according to (4), the results of which are seen in the same table. These values are all very low, which is logical considering there are only eight highly directional TX antennas. The dominating coupling is S_{51} since the TX antenna lobes are pointing towards each other.

TABLE V. Average channel gain, with horizontal and vertical polarizations, respectively at both ends. The total disturbance level for each polarization is given as D_r.

$Sx1$	**H-H** $[dB]$	**V-V** $[dB]$
S_{21}	-79.5	-72.1
S_{31}	-78.8	-84.7
S_{41}	-64.5	-72.8
S_{51}	-58.4	-58.8
D_r	-56.6	-58.1

Next we analyze how the received power levels are affected by the presence of a test object. Table VI shows the changes in the power levels as a result of placing the test objects in the test zone. All values are averaged within the frequency band. The changes are due to scattering by the test object,

TABLE VI. CHANGE IN POWER LEVELS DUE TO PRESENCE OF A TEST OBJECT. FOR TEST OBJECT CAR, ONLY POSITION A.

ΔS_{x1}	Laptop		Volvo C30		Volvo S60		Volvo XC90	
	H-H $[dB]$	V-V $[dB]$	H-H $[dB]$	V-V $[dB]$	H-H $[dB]$	V-V $[dB]$	H-H $[dB]$	V-V $[dB]$
ΔS_{21}	+3.6	+0.3	+0.4	-0.2	-1.7	+1.5	+0.3	+1.3
ΔS_{31}	-0.3	+1.0	-3.3	+5.1	+1.4	-1.4	+2.3	-1.3
ΔS_{41}	-5.0	+5.4	+1.6	+0.1	+0.8	-1.0	+1.3	-1.2
ΔS_{51}	+3.1	-1.0	+3.5	-0.3	+1.5	-0.9	-9.1	-5.8

and the amount of scattered power can thereby be quantified. The scattered power does not necessarily cause any problems in actual OTA multi-probe measurements, because they might only be reflected away from the test zone and not towards the test objects antenna. However, these results are useful to get a complete picture of the disturbance levels, and for assessing the necessity of placing the OTA multi-probe setup in an open area or an anechoic chamber. Should the reflection from the test object be high, it is also reason for caution when measuring on other test objects with a bigger size where the reflected power might find its way into the car antenna.

All S-parameters have a LOS signal path when the test object is in place except for the measurement with the Volvo XC90. For the S_{51} measurement the only possibility of a specular reflection on a large surface is the roof on one of the cars. This means that in most cases, reflections from edges, diffuse scattering, multiple reflections, and diffractions, are the reasons for changes in received power, compared to the case with NO test object. From the results, it is concluded that there are strong reflection/diffraction from the test objects body. The most critical parameter is ΔS_{51} since S_{51} has much higher contribution to the disturbance level compared to the other. If the delta values are positive the disturbance levels are increased for the case with the test object. The largest positive value of ΔS_{51} for the measurements is the value for horizontal polarization for Volvo C30, +3.5 dB. This means that the total disturbance value has increased from -56.6 dB to -53.7 dB, which in practice is negligible.

To understand the influence on the test signal when a test object is placed in the test zone the impulse response was analysed, see Fig. 14 and Fig. 15. The ground reflection is clearly visible for NO test object but also with the Laptop since this test object is standing on a wooden and cardboard stand 1.05 m above ground. Otherwise the impulse responses with and without a test object have similar shapes. By this we conclude that even though there are strong reflections/diffractions these multipath components are reflected away from the test zone and not towards the antenna of the test objects.

VI. SUMMARY AND CONCLUSIONS

In this paper we have presented three experiments on an Over-the-Air Multi-Probe Setup for Cars at 5.9 GHz: a measurement system analysis, channel sounder measurements and probe coupling measurements. In the analysis of the test results the main focus has been to investigate the four specific issues identified; precision, realization of wireless communication channel, coupling between TX antennas, and the influence of the test object size. The MSAs show that the precision of the chosen response metrics as defined by expanded uncertainty, u_e is below ± 0.86 dB. When the difference between performance on the RX antennas are larger than u_e the MSAs also show that the repeatability and reproducibility are under control, $G_{R\&R} < 9\,\%$. With the presented setup with eight TX antennas the analysis of the channel sounder measurements shows that generation of a desired wireless communication channel is possible. The coupling between the TX antennas in the multi-probe ring seems not to be a big problem since the disturbance level from other TX antennas than the transmitting TX antenna is -56.6 dB for horizontal polarization and -58.1 dB for vertical polarization. The size of the test object has an influence on the disturbance level, but only to a small degree. There was a maximum increase in power of +3.5 dB for horizontal polarization on the small car, Volvo C30. The analysis of the impulse response from

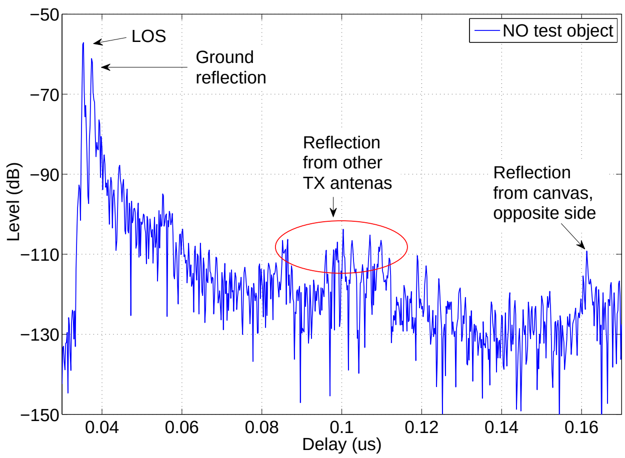

Fig. 14. Impulse response of S_{51} for NO test object with vertical polarization at the Open area (tent).

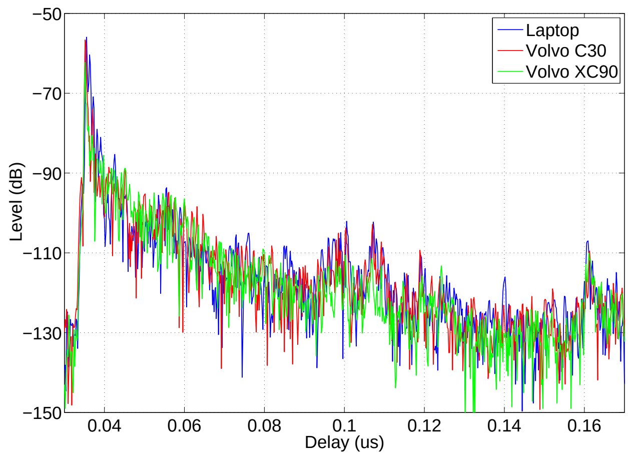

Fig. 15. Impulse response of S_{51} for the Laptop, the Volvo C30 and the Volvo XC90 with vertical polarization and position A of the cars. All measurements were performed at the Open area (tent).

the coupling measurements and the MSAs shows that the reflected/diffracted multipath components are reflected away from the test zone. Before performing active communication tests with the studied MPS equipment, an assessment should be made of the allowed disturbance level. This is then compared with the presented results, to assess the viability of the MSP method.

Three drawbacks with the presented OTA multi-probe setup should be mentioned: 1) the number of multipath components of the simulated channel is bounded by the number of TX antennas, 2) the angle of arrivals of the multipath components are constant and limited to the TX antenna placement in the ring, 3) the Doppler frequency and delay are time-invariant. These limitations are not general with all channel emulation techniques in OTA multi-probe setups.

The conclusion we make from all above is that the OTA multi-probe setup is a way forward for an efficient way of characterizing today's wireless communication systems for cars. By this we will continue our research in this field to extend it to other scenarios, active signaling testing, and to other wireless communication technologies for cars. Simulating the wave propagation inside the ring has already started. Investigation of different number of TX antennas is still a future outlook.

VII. Acknowledgement

This work was funded by the Swedish Governmental Agency for Innovation Systems - VINNOVA, through the project Wireless Communication in Automotive Environment. We also would like to thank Dimitrios Vlastaras for his help during the channel sounder measurements.

References

[1] "IEEE Standard for Information Technology – Telecommunications and information exchange between systems – Local and metropolitan area networks – Specific requirements – Part 11: Wireless LAN Medium Access Control (MAC) and Physical Layer (PHY) Specifications," *IEEE Std 802.11-2012*, March 2012.

[2] "Intelligent Transport Systems (ITS); Vehicular Communications; Basic Set of Applications," *ETSI TR 102 638 V1.1.1*, 2009.

[3] C. Mecklenbrauker, A. Molisch, J. Karedal, F. Tufvesson, A. Paier, L. Bernado, T. Zemen, O. Klemp, and N. Czink, "Vehicular channel characterization and its implications for wireless system design and performance," *Proceedings of the IEEE*, vol. 99, Issue: 7, pp. 1189 – 1212, July 2011.

[4] M. Rumney, R. Pirkl, M. H. Landmann, and D. A. Sanchez-Hernandez, "MIMO over-the-air research, development, and testing," *Hindawi International Journal of Antennas and Propagation*, vol. 2012, p. 8, May 2012.

[5] P. Corona, G. Latmiral, E. Paolini, and L. Piccioli, "Use of a reverberating enclosure for measurements of radiated power in the microwave range," *IEEE Transactions on Electromagnetic Compatibility*, vol. EMC-18, pp. 54–59, 1976.

[6] H. Arai and T. Urakawa, "Radiation power measurement using compact shield box," *Proceedings of ISAP*, pp. 1005–1008, 1996.

[7] J. D. Sánchez-Heredia, P. Hallbjörner, J. F. Valenzuela Valdés, T. Bolin, and A. M. Martínez-González, "Differences in user influence on MIMO handset antenna performance in reverberation chamber," *Hindawi International Journal of Antennas and Propagation*, 2012.

[8] E. L. Caples, K. E. Massad, and T. R. Minor, "A UHF channel simulator for digital mobile radio," *IEEE Transactions on Vehicular Technology*, vol. 29, pp. 281–289, 1980.

[9] C. Park, J. Takada, K. Sakaguchi, and T. Ohira, "Spatial fading emulator for base station using cavity-excited circular array based on espar antenna," in *Proceedings of 60th IEEE Vehicular Technology Conference (VTC)*, vol. 1, 26-29 September 2004, pp. 256–260.

[10] P. Hallbjörner, Z. Ying, M. Håkansson, C. Wingqvist, T. Anttila, and J. Welinder, "Multipath simulator for mobile terminal antenna characterisation," *IET Microwaves, Antennas and Propagation*, vol. 4, Issue 2, pp. 743–750, 2010.

[11] W. Fan, X. Carreño Bautista de Lisbona, F. Sun, J. Ødum Nielsen, M. Bergholz Knudsen, and G. Frølund Pedersen, "Emulating spatial characteristics of MIMO channels for OTA testing," *IEEE Transactions on Antennas and Propagation*, vol. 61, No. 8, pp. 4306–4314, August 2013.

[12] Y. Jing, X. Zhao, H. Kong, S. Duffy, and M. Rumney, "Two-stage over-the-air (OTA) testmethod for LTE MIMO device performance evaluation," *International Journal of Antennas and Propagation*, vol. 2012, Article ID 572419, 6 pages, 2012.

[13] M. Nilsson, P. Hallbjörner, N. Arabäck, B. Bergqvist, and F. Tufvesson, "Multipath propagation simulator for V2X communication tests on cars," in *Proceedings of 7th European Conference on Antennas and Propagation (EuCAP)*, 8-12 April 2013, pp. 1342 – 1346.

[14] "Satimo." [Online]. Available: http://www.satimo.com/content/antenna-measurement-systems-0 [14-Dec-2014]

[15] P. Hallbjörner, "Design rules for multipath simulator antenna array," SP Technical Research Institute of Sweden, ISBN 978-91-86319-93-9, ISSN 0284-5172, Tech. Rep., 2010.

[16] W. Fan, I. Szini, M. D. Foegelle, J. Ø. Nielsen, and G. F. Pedersen, "Measurement uncertainty investigation in the multi-probe OTA setups," in *8th European Conference on Antennas and Propagation (EuCAP)*, 6-11 April 2014, pp. 1068 – 1072.

[17] P. Kyösti, T. Jämsä, and J.-P. Nuutinen, "Channel modelling for multiprobe Over-the-Air MIMO testing," *Hindawi International Journal of Antennas and Propagation*, vol. 2012, p. 11, March 2012.

[18] J. Toivanen, T. Laitinen, V.-M. Kolmonen, and P. Vainikainen, "Reproduction of arbitrary multipath environments in laboratory conditions," *IEEE Transactions on Instrumentation and Measurement*, vol. 60 No. 1, pp. 275–281, January 2011.

[19] W. Fan, J. Nielsen, O. Franek, X. Carreño, J. Ashta, M. Knudsen, and G. Pedersen, "Antenna pattern impact on MIMO OTA testing," *IEEE Transactions on Antennas and Propagation*, vol. 61 No.11, pp. 5714–5723, November 2013.

[20] T. Laitinen, P. Kyösti, J.-P. Nuutinen, and P. Vainikainen, "On the number of OTA antenna elements for planewave synthesis in a MIMO-OTA test system involving a circular antenna array," in *Proceedings of the 4th European Conference on Antennas and Propagation (EuCAP)*, 12-16 April 2010, pp. 1–5.

[21] L. Rudant, C. Delaveaud, and M. Abou-El-Anouar, "Synthesizing realistic environments in an anechoic chamber," in *Proceedings of 3rd European Conference on Antennas and Propagation*, March 2009, pp. 221–225.

[22] P. Hallbjörner, J. D. Sánchez-Heredia, P. Lindberg, A. M. Martínez-González, and BolinT., "Multipath simulator measurements of handset dual antenna performance with limited number of signal paths," *IEEE Transactions on Antennas and Propagation*, vol. 60, No.2, pp. 682–688, 2012.

[23] J. D. Sánchez-Heredia, P. Hallbjörner, T. Bolin, and A. M. Martínez-González, "HSDPA throughput performance with limited number of signal paths," *IEEE Antennas and Wireless Propagation Letters*, vol. 11, pp. 484–487, 2012.

[24] T. Bolin, D. Pugachov, M. Mora-Andreu, and P. Hallbjörner, "MPS results on LTE MIMO OTA 2013 round robin tests," in *Proceedings of the 8th European Conference on Antennas and Propagation (EuCAP)*, 6-11 April 2014, pp. 4330–4334.

[25] Abbas, T. and Karedal, J. and Tufvesson, F. and Paier, A. and Bernado, L. and Molisch, A.F., "Directional analysis of vehicle-to-vehicle prop-

agation channels," in *Proceeding of 73rd IEEE Vehicular Technology Conference (VTC)*, 15-18 May 2011, pp. 1–5.

[26] O. Renaudin, V.-M. Kolmonen, P. Vainikainen, and C. Oestges, "Wideband measurement-based modeling of inter-vehicle channels in the 5-GHz band," *Vehicular Technology, IEEE Transactions on*, vol. 62, no. 8, pp. 3531–3540, Oct 2013.

[27] T. A. Laitinen, J. Ollikainen, C. Icheln, and P. Vainikainen, "Rapid spherical 3-D field measurement system for mobile terminal antennas," in *Proceedings of IMTC 2003 - Instrumentation and Measurement Technology Conference*, vol. 2, 20-22 May 2003, pp. 968 – 972.

[28] W. Fan, F. Sun, P. Kyösti, J. Nielsen, X. Carreño, M. Knudsen, and G. Pedersen, "3D channel emulation in multi-probe setup," *Electronics Letters*, vol. 49, No. 9, 25 April 2013.

[29] R. K. Sharma, C. Schneider, W. Kotterman, G. Sommerkorn, P. Grosse, F. Wollenschlager, G. Del Galdo, M. A. Hein, and R. S. Thoma, "Over-the-air testing of car-to-car and car-to-infrastructure communication in a virtual electromagnetic environment," in *Proceedings of 39th Annual Conference of the IEEE - Industrial Electronics Society, (IECON)*, 10-13 November 2013, pp. 6897 – 6902.

[30] A. Sleeper, *Design for Six Sigma Statistics, 59 Tools for Diagnosing And Solving Problems in Dffs Initiatives*, A. Sleeper, Ed. McGraw-Hill Professional, 2006.

[31] "Evaluation of measurement data - Guide to the expression of uncertainty in measurement," *ISO/IEC - JCGM 100:2008*, 2008.

[32] D. C. Corporation, F. M. Company, and G. M. Corporation, *Measurement System Analysis*, 2nd ed., D. C. Corporation, F. M. Company, and G. M. Corporation, Eds. Automotive Industry Action Group (AIAG), 1995.

[33] "Electromagnetic compatibility and Radio spectrum Matters (ERM); Uncertainties in the measurement of mobile radio equipment characteristics; Part 1," *ETSI TR 100 028-1*.

[34] T. Ödman and P. Hallbjörner, "Vivaldi antenna with low frequency resonance for reduced dimensions," in *Proceedings of 7th European Conference on Antennas and Propagation (EuCAP)*, 8-12 April 2013, pp. 2457 – 2459.

[35] "Specification for radio disturbance and immunity measuring apparatus and methods Part 1-4: Radio disturbance and immunity measuring apparatus Antennas and test sites for radiated disturbance measurements," *IEC CISPR 16-1-4*, vol. 3.0, 2010.

[36] R. Thomä, D. Hampicke, A. Richter, G. Sommerkorn, A. Schneider, U. Trautwein, and W. Wirnitzer, "Identification of time-variant directional mobile radio cahannels," *IEEE Transactions on instrumentation and measurement*, vol. 49, pp. 357–364, April 2000.

[37] P. Hallbjörner, "Measurement uncertainty in multipath simulators due to scattering within the antenna array theoretical model based on mutual coupling," *IEEE Antennas and Wireless Propagation Letters*, vol. 9, pp. 1103–1106, 2010.

Mikael Nilsson (M'09) received his B.Sc. degree in Electrical Engineering - Radio electronics at Växjö University, Sweden, in 1997. From 1997 through 2003 he worked mostly as consultant within telecom and space industry. In 2003 he joined Volvo Cars and he have had different positions within the company. Since 2011 he hold the position as industrial Ph.D. student enrolled at Lund University, Sweden, department of Electrical and Information Technology, and his principle research areas are channel characterization of the 5.9 GHz band and measurement systems, namely the Over-the-Air mutlti-probe setup for cars. Also since 2012 he holds the position as Technical Expert - Wireless Communication within Volvo Cars. Mikael Nilsson is dedicated to the Six Sigma methodology and has teaching several Design for Six Sigma and Green Belt courses within Volvo Cars.

Paul Hallbjörner was born in Uppsala, Sweden, in 1966. He received his B.Sc. in 1988, M.Sc. in 1995, and Ph.D. in 2005, all in Electrical Engineering, from Chalmers University of Technology in Gteborg, Sweden. He has worked in the telecom industry since 1989, with pre-production engineering, product development, and research, mainly in the field of antennas and microwave technology. He is the author of more than 90 scientific publications, and is the inventor to ten patents. He is retired since 2014.

Niklas Arabäck was born in Sweden, in 1977. He received B.Sc degree in electronic from Högskolan i Borås, in 2008. From 2008 to 2011 he was an EMC engineer at SP Technical Research Institute of Sweden. Currently he is a research engineer at the Electronics Department - EMC at SP Technical Research Institute of Sweden. His primary research interests are in multipath propagation for vehicular applications.

Björn Bergqvist work as a technical expert in EMC and RF communication at Volvo Car Corporation. He has a long experience in practical EMC project management and testing within the automotive industry. Björn is also teaching Six Sigma and Design for Six Sigma. Today Björn mainly works with early concept development and research projects.

Taimoor Abbas (S'09, M'14) received his M.Sc. degree in electronics from Quaid-i-Azam University Islamabad, Pakistan, in 2006, and M.S. degree in wireless communications and Ph.D. degree in radio systems from the department of Electrical and Information Technology, Lund University, Sweden, in 2009 and 2014, respectively. He has been with Ericsson for his master thesis internship. He is now at Volvo Cars. His current research areas include C-ITS, MIMO, 5G systems, and estimation and modeling of radio channels.

Fredrik Tufvesson received his Ph.D. in 2000 from Lund University in Sweden. After two years at a startup company, he joined the department of Electrical and Information Technology at Lund University, where he is now professor of radio systems and is heading the wireless propagation group. His main research interests are channel modeling and characterization for wireless communication, with applications in various areas such as radio based positioning, distributed antenna systems, massive MIMO, UWB, mm wave, and vehicular communication systems.